Hum Genet
DOI 10.1007/s00439-012-1197-8

ORIGINAL INVESTIGATION

Further characterization of *ATP6V0A2*-related autosomal recessive cutis laxa

Björn Fischer · Aikaterini Dimopoulou · Johannes Egerer · Thatjana Gardeitchik · Alexa Kidd · Dominik Jost · Hülya Kayserili · Yasemin Alanay · Iliana Tantcheva-Poor · Elisabeth Mangold · Cornelia Daumer-Haas · Shubha Phadke · Reto I. Peirano · Julia Heusel · Charu Desphande · Neerja Gupta · Arti Nanda · Emma Felix · Elisabeth Berry-Kravis · Madhulika Kabra · Ron A. Wevers · Lionel van Maldergem · Stefan Mundlos · Eva Morava · Uwe Kornak

Received: 20 June 2012 / Accepted: 21 June 2012

Abstract Autosomal recessive cutis laxa (ARCL) syndromes are phenotypically overlapping, but genetically heterogeneous disorders. Mutations in the *ATP6V0A2* gene were found to underlie both, autosomal recessive cutis laxa type 2 (ARCL2), Debré type, and wrinkly skin syndrome (WSS). The *ATP6V0A2* gene encodes the a2 subunit of the V-type H^+-ATPase, playing a role in proton translocation, and possibly also in membrane fusion. Here, we describe a highly variable phenotype in 13 patients with ARCL2, including the oldest affected individual described so far, who showed strikingly progressive dysmorphic features and heterotopic calcifications. In these individuals we identified 17 *ATP6V0A2* mutations, 14 of which are novel. Furthermore, we demonstrate a localization of ATP6V0A2 at the Golgi-apparatus and a loss of the mutated ATP6V0A2 protein in patients' dermal fibroblasts. Investigation of brefeldin A-induced Golgi collapse in dermal fibroblasts as well as in HeLa cells deficient for ATP6V0A2 revealed a delay, which was absent in cells deficient for the ARCL-associated proteins GORAB or PYCR1. Furthermore, fibroblasts from patients with *ATP6V0A2* mutations displayed elevated TGF-β signalling

J. Egerer and T. Gardeitchik contributed equally. B. Fischer and A. Dimopoulou contributed equally.

Electronic supplementary material The online version of this article (doi:10.1007/s00439-012-1197-8) contains supplementary material, which is available to authorized users.

B. Fischer · A. Dimopoulou · J. Egerer · D. Jost · S. Mundlos · U. Kornak (✉)
Institut fuer Medizinische Genetik und Humangenetik, Charité-Universitaetsmedizin Berlin, Berlin, Germany
e-mail: uwe.kornak@charite.de

J. Egerer · S. Mundlos · U. Kornak
FG Development and Disease, Max-Planck-Institut fuer Molekulare Genetik, Berlin, Germany

T. Gardeitchik · E. Morava
Department of Pediatrics, Radboud University Nijmegen Medical Center, Nijmegen, The Netherlands

A. Kidd · E. Felix
Central and Southern Regional Genetic Services, Wellington Hospital, Wellington South, New Zealand

H. Kayserili
Medical Genetics Department, Istanbul Medical Faculty, Istanbul University, Istanbul, Turkey

Y. Alanay
Department of Child Health and Diseases, Acibadem University, Istanbul, Turkey

I. Tantcheva-Poor
Department of Dermatology, University of Cologne, Cologne, Germany

E. Mangold
Institute of Human Genetics, University of Bonn, Bonn, Germany

C. Daumer-Haas
Prenatal Medicine Munich, Munich, Germany

S. Phadke
Department of Medical Genetics, Sanjay Gandhi Postgraduate Institute of Medical Sciences, Lucknow, India

R. I. Peirano · J. Heusel
Beiersdorf AG, R&D, Skin Research Center, Unnastrasse 48, 20253 Hamburg, Germany

C. Desphande
Department of Clinical Genetics, Guy's Hospital, London, UK

N. Gupta · M. Kabra
Department of Pediatrics, All India Institute of Medical Sciences, New Delhi, India

Published online: 08 July 2012

and increased TGF-β1 levels in the supernatant. Our current findings expand the genetic and phenotypic spectrum and suggest that, besides the known glycosylation defect, alterations in trafficking and signalling processes are potential key events in the pathogenesis of *ATP6V0A2*-related ARCL.

Introduction

Cutis laxa (CL), recognizable either by loose, redundant skin folds or skin wrinkling, is a phenotypic feature of a number of syndromic disorders. While in most cases a general involvement of connective tissues is evident, manifestations in other organ systems are variable and depend on the subtype. Cutis laxa comprises X-linked, autosomal dominant and autosomal recessive forms. Among these different forms autosomal recessive cutis laxa (ARCL) is the most prevalent type and appears to be the most heterogeneous in terms of phenotypic features and underlying molecular defects (Morava et al. 2009a). At the more severe end of the autosomal recessive cutis laxa phenotypic spectrum lies the ARCL type I (ARCL1; OMIM 219100) characterized by pulmonary emphysema, cardiovascular problems, and gastrointestinal and vesicourinary tract diverticuli. It was found to primarily result from homozygous mutations in fibulin-5 (*FBLN5*) (Loeys et al. 2002). Further studies revealed that mutations in the gene encoding for EGF-containing fibulin-like extracellular matrix protein 2 gene (*EFEMP2*) [formerly fibulin-4 (*FBLN4*)] can lead to an even more severe phenotype (Hoyer et al. 2009; Hucthagowder et al. 2006). A form of ARCL type I can also be caused by *LTBP4* mutations (Urban et al. 2009). ARCL type II comprises a number of overlapping phenotypes. Mutations in *GORAB*, encoding a newly identified golgin, were found to cause gerodermia osteodysplastica (GO; OMIM 231070) (Hennies et al. 2008). In contrast to other types of ARCL, GO patients have an increased risk of spontaneous bone fractures due to osteoporosis, suggestive facial features with jaw hypoplasia but seldom neurological involvement (Noordam et al. 2009). Metabolic investigations, such as protein glycosylation analysis, are normal (Morava et al. 2009a; Rajab et al. 2008). Another form of ARCL, MACS syndrome (MACS; OMIM 613075), is due to mutations in *RIN2*, a Rab5 effector. Clinical hallmarks are macrocephaly, alopecia, scoliosis, typical facial coarsening, thick lips, mild alterations in serum protein glycosylation and variable mental retardation (Albrecht et al. 2011; Basel-Vanagaite et al. 2009). De Barsy syndrome (DBS; OMIM 219150) has been referred to as ARCL type III and is characterized by a progeroid appearance with short stature, corneal clouding, hypotonia and pronounced mental retardation (de Barsy et al. 1968; Kunze et al. 1985). The molecular defect in DBS is not fully clear. Recently, mutations in *PYCR1* (ARCL2B; OMIM 612940), encoding a mitochondrial protein involved in de novo proline biosynthesis, were found in patients initially diagnosed as having wrinkly skin syndrome, gerodermia osteodysplastica or de Barsy syndrome (Reversade et al. 2009). Another neurocutaneous disorder showing features overlapping with de Barsy syndrome is caused by mutations in *ALDH18A1*, coding for another enzyme involved in proline biosynthesis (Bicknell et al. 2008).

Mutations in *ATP6V0A2*, encoding the a2 subunit of the H^+-ATPase, were found to cause cutis laxa with generalized skin wrinkling, delayed closure of the anterior fontanelle, downslanting palpebral fissures, a varying degree of developmental delay, cobblestone-like brain malformations and occasionally a severe neurodegenerative phenotype with seizures and dementia (Kornak et al. 2008; Morava et al. 2005; Van Maldergem et al. 2008). A unique feature is a combined defect of N- and O-glycosylation of serum proteins (CDG type II) (Kornak et al. 2008; Mohamed et al. 2011b; Morava et al. 2005). The disorder was named ARCL Debré type and also classifies as a congenital disorder of glycosylation (ATP6V0A2-CDG). The disease appears to have a milder variant referred to as wrinkly skin syndrome.

The V-Type H^+-ATPase is composed of two multisubunit domains, V_0 and V_1, and is involved in pH homeostasis and intracellular transport (Beyenbach and Wieczorek 2006; McHenry et al. 2010). Both domains are connected by the a subunit, which is composed of 8–9 transmembrane helices and a long cytoplasmic N-terminal domain (Jefferies et al. 2008). Four closely related paralogs exist for the a subunit. Except for a4, the other three a

A. Nanda
Pediatric Dermatology Unit, Asad Al-Hamad Dermatology Center, Al-Sabah Hospital, Kuwait City, Kuwait

E. Berry-Kravis
Department of Pediatrics, Neurological Sciences and Biochemistry, Rush University Medical Center, Chicago, IL, USA

R. A. Wevers
Laboratory of Genetic, Endocrine and Metabolic Diseases, Radboud University Nijmegen Medical Centre, Nijmegen, The Netherlands

L. van Maldergem
Cutis laxa, Debré type Study Group, Centre de Génétique Humaine, Centre Hospitalier Universitaire, Université de Franche-Comté, 25000 Besançon, France

S. Mundlos
Berlin-Brandenburg Center for Regenerative Therapies, Charité-Universitaetsmedizin Berlin, Berlin, Germany

subunits are expressed broadly and in an overlapping manner. Mutations in *ATP6V0A2*, *-A3 (TCIRG1)* and *-A4* are known to cause human hereditary disorders (Guillard et al. 2009). Different types of mutations affecting multiple domains have been described in ATP6V0A2 (Hucthagowder et al. 2009; Kornak et al. 2008). In most cases a loss-of-function effect is likely, but has not been proven directly. Mutations in *ATP6V0A2* result in different cellular phenotypes. Skin fibroblasts from ARCL2A patients show impaired maturation and secretion of tropoelastin. Fragmentation of the Golgi-apparatus, a delayed Golgi collapse upon treatment with brefeldin A (BFA), and accumulation of abnormal cargo vesicles indicate that different cellular trafficking routes are affected by ATP6V0A2 dysfunction. As a possible result of these events apoptosis rates are increased in cells deficient for ATP6V0A2 (Hucthagowder et al. 2009). The present study focuses on clinical, genetic and molecular findings in patients carrying novel mutations in the *ATP6V0A2* gene.

Materials and methods

Patients

In this study we investigated 13 patients, who fulfilled the major diagnostic criteria for *ATP6V0A2*-related cutis laxa. These criteria included: generalized skin wrinkling, delayed closure of the anterior fontanel and a typical face with downslanting palpebral fissures and a broad nasal root. Consent for molecular studies was obtained from all individuals involved in this study or from their legal representatives. The Charité Medical University ethics committee approved the study. The study was performed according to the declaration of Helsinki. Written consent for publication of photographs was given by the patients or their legal representatives.

ATP6V0A2 mutation screening

Sequencing of all exons and the flanking intron regions of the *ATP6V0A2* (NM_012463) gene was performed as described previously (Kornak et al. 2008) in each tested individual or the parents as obligate heterozygous carriers. All mutations were tested for segregation in the patient's families (if available). Sequencing reaction was performed with the BigDye Terminator cycle sequencing kit (Applied Biosystems, Foster City, CA), and run on a 3730 DNA Analyzer (Applied Biosystems, Foster City, CA). Sequences were evaluated and compared to reference sequences with DNASTAR (DNASTAR Madison, USA) The molecular diagnostic tests were performed in an accredited laboratory (No.: DAP-ML-3869.00 (ISO 15189:2003 and ISO/IEC 17025:2005). Functional effects of missense mutations were examined by assessing evolutionary conservation of the affected residues by BLAST alignment and interspecies comparison using Mutation Taster (Schwarz et al. 2010).

Cell culture

Human skin fibroblasts were cultivated in DMEM (Lonza) supplemented with 10 % fetal calf serum (FCS) (Gibco), 1 % Ultraglutamine (Lonza) and 1 % penicillin/streptomycin (Lonza). HeLa cells were cultivated in the same medium without penicillin/streptomycin and supplemented with 5 % FCS. Cells were grown at 37 °C and 5 % CO_2.

RNA interference (RNAi)

In 6-well plates 9,000 cells/cm^2 were seeded 16 h before siRNA transfection on glass coverslips. For transfection 200 nM of control (siRNA ID: AM4635, Ambion), ATP6V0A2 (siRNA ID: 20328, Ambion), GORAB (siRNA ID # s40928, Ambion), PYCR1 (siRNA ID # s194735, Ambion) siRNA oligonucleotides were transfected by INTERFERin (Polyplus-transfection). After 8 h a second transfection was done. Cells were grown for another 64 h and subsequently analysed. Knock-down efficiency was verified by quantitative PCR.

Quantitative PCR

Cells were lysed with Trizol® and total RNA was prepared by a standard RNA extraction protocol. Total cDNA was transcribed by RevertAidTM H Minus First Strand cDNA Synthesis Kit (Fermentas) using random hexamer primer. Quantitative PCR was performed with SYBR green (Invitrogen) on ABI Prism 7500 (Applied Biosystems, Foster City, USA). Data were analysed by ABI Prism SDS Software package by using the $\Delta\Delta C_t$ method. Normalization was done according to GAPDH levels and graphical output was created by Excel (Microsoft, Seattle). All primer sequences are available on request.

Immunofluorescence

Cells grown on glass coverslips were washed three times in phosphate-buffered saline (PBS), fixed for 10 min at 4 °C in 4 % paraformaldehyde and permeabilized with 0.1 % saponin in 3 % BSA in 1× PBS for 10 min. For detection of ATP6V0A2 we used an antibody previously described and kindly provided by Dr. E. Ntrivalas (Ntrivalas et al. 2007). As Golgi markers we used mouse anti-GM130 (BD Transduction Laboratories), rabbit anti-giantin (Covance). Secondary antibodies were anti-mouse IgG Alexa Fluor

555 (Invitrogen, Molecular Probes) and an anti-rabbit IgG Alexa Fluor 488 (Invitrogen, Molecular Probes). DNA was stained by DAPI and cells were mounted in Fluoromount G (Scientific Services). Images were collected by an LSM 510 meta (Carl Zeiss, Göttingen, Germany) with a ×63 Plan Apochromat oil immersion objective.

Immunoblot

Cells were lysed in membrane lysis buffer (50 mM NaF, 30 mM NaPPi, 5 mM EDTA, 1 % Triton-X 100 in 1× TBS) supplemented with Complete proteinase inhibitor (Roche). Protein concentrations were determined using a BCA assay kit (Pierce). 10 µg of protein per lane were separated by 10 % SDS PAGE and subsequently transferred to nitrocellulose membranes. After tank blotting overnight membranes were blocked in 5 % block milk (5 g dry milk powder, 0.2 % NP-40 in 1× TBS), probed with an antibody against phospho-Smad2 (Cell Signaling) and with antibodies against GAPDH (Ambion) or Smad2 (Cell Signaling). Membranes were washed and incubated with HRP-conjugated secondary antibodies. Signals were detected using ECL reaction (Amersham). All blots were performed at least three times with different cell lysates. Densitometric quantification of the results was performed using the Image J Software package.

Brefeldin A-induced Golgi collapse

Patient skin fibroblasts or HeLa cells treated with siRNA were incubated with 5 µg/ml brefeldin A (Sigma). Coverslips were fixed and stained after indicated time points. Pictures were taken with a fluorescence microscope (BX60, Olympus). At least 250 cells per sample were counted. High-resolution pictures were collected using an LSM 510 meta (Carl Zeiss, Göttingen, Germany) with a ×63 Plan Apochromat oil immersion objective.

TGF-β 1 ELISA

Patient and control fibroblasts were seeded at a density of 2×10^6 cells per six well to directly reach confluency. After 2 days the medium was removed and the cells were incubated with starvation medium (DMEM supplemented with 1 % Ultraglutamine and 5 mg/ml BSA) for an additional 24 h. After 3 days this medium was collected in polypropylene tubes. Cell debris was removed by centrifugation and latent TGF-β1 was acid activated since otherwise no active TGF-β1 was detectable. An ELISA (R&D) was performed according to manufacturer's instructions. All obtained fluorescence values were corrected against total protein concentration.

Results

Clinical findings

We analyzed 13 patients that fulfilled the clinical criteria for wrinkly skin syndrome or ARCL2, Debré type (Table 1) (Fig. 1a–h). Clinical evaluation showed deep palmar and plantar creases and an abnormal distribution of subcutaneous fat tissue in several cases. In contrast to *ALDH18A1*- and *PYCR1*-related ARCL, no intrauterine growth retardation (IUGR) was noted in our patient group. Furthermore, a combined N-glycosylation (type 2) and O-glycosylation defect differentiates *ATP6V0A2*-related ARCL from other CL forms. In the present study we found altered glycosylation patterns in all patients tested (Table 1).

Patient 2, who is the oldest affected individual in our series, developed a so far undescribed dysmorphism. At one and five years of age he only showed the typical facial features of *ATP6V0A2*-related ARCL (Fig. 1a, b). However, at the age of 40 years he displayed a striking facial coarsening (Fig. 1c, d). In addition, a progressive kyphoscoliosis and a chronic luxation of the right shoulder were evident (Fig. 1c–e). Radiological imaging also showed pathological calcifications in tissue surrounding the femur (Fig. 1f, g) and the malleoli (data not shown), which remained unchanged in the follow-up. He had not only a mild to moderate mental retardation, which was also present in the majority of the cases (Table 1), but also developed seizures in the second decade and increasing behavioural problems in the fifth decade. Patient 8, the only one of the three affected individuals from India for whom clinical pictures were available, showed a typical manifestation for *ATP6V0A2*-related ARCL (Fig. 1h, i). Patients 2 and 8 both had an ophthalmic pterygium (Fig. 1j, k), which is unusual at least at the young age of patient 8.

Patient 1 showed a cobblestone-like brain dysgenesis pattern in exactly the same frontotemporal distribution as described before in *ATP6V0A2*-related cutis laxa patients, and a typical enlargement of the Virchow space (Mohamed et al. 2011b; Morava et al. 2009b). No MRI data were available for the other patients.

ATP6V0A2 mutation screening

The clinical appearance of all 13 patients indicated an *ATP6V0A2*-associated cutis laxa phenotype. Mutation screening in those individuals identified 17 different *ATP6V0A2* mutations: one mutation of the start codon, three missense mutations, three nonsense mutations, three splice site mutations, three in-frame deletions, and four frameshift mutations (Table 1; Fig. 2a, upper part). Mutation p.R63X (patients 9, 11) and p.E646_685del (patient

Table 1 Summary of molecular genetic, biochemical, cellular and clinical findings

Patient no.	Origin	Consanguinity	Mutation			BFA Effect	CDG	Clinical features				Mutation Known
			cDNA	Status	Protein			Wrinkled skin	Joint laxity	Large fontanel	Mental retardation	
1	Poland	No	c.708_713delCAAGGT	Het	p.K237_V238del	+	+	+	+	+	−	Novel
			c.2015T>A	Het	p.L672X							
2	New Zealand	No	c.117+1delG	Het	splicing	+	+	++	++	+	++	Novel
3	India	nd	c. 2355-2361delTGGCGTC	Hom	p.Y785fsX800	nd	nd	++	++	+	−	Novel
4	India	nd	c.430_432delCAG	Hom	p.E144del	nd	nd	++	−	++	−	Novel
5	Kuwait	No	c.2055+2dupT	Het	splicing	+	+	++	++	a	+	Novel
			c.2432T>C	Het	p.L811P							
6	Turkey	Yes	c.100_101insA	Hom	p. V476SfsX499	nd	nd	+++	−	b	nd	Novel
7	UK	nd	c.600delC	Het	p.T200fsX220	nd	nd	++	+	+	++	Novel
			c.1246G>A	Het	p.G416R							
8	India	Yes	c.16_17dupC	Hom	p.F5fsX54	nd	nd	++	++	+	nd	Novel
9	Turkey	Yes	c.187C>T	Hom	p.R63X	nd	nd	++	++	+	nd	Kornak et al. (2008)
10	Afghanistan	Yes	c.1A>T	Hom	p.M1?	+	+	+++	nd	+	−	Novel
11	Turkey	nd	c.187C>T	Hom	p.R63X	nd	nd	++	++	+	+	Kornak et al. (2008)
12	Turkey	Yes	c.1936_2055del	Hom	p.E646_685del	nd	+	+	++	nd	+−	Hucthagowder et al. 2009
13	Italy	No	c.1326+1G>A	Het	Splicing	nd	+	+	+	+	+−	Novel
			c.2287C>T	Het	p.H763Y							

− absent, +− very mild, + mild, ++ moderate, +++ severe, *a* closure of fontanel at 26 months, *b* closure of fontanel at 48 months, *nd* not determined

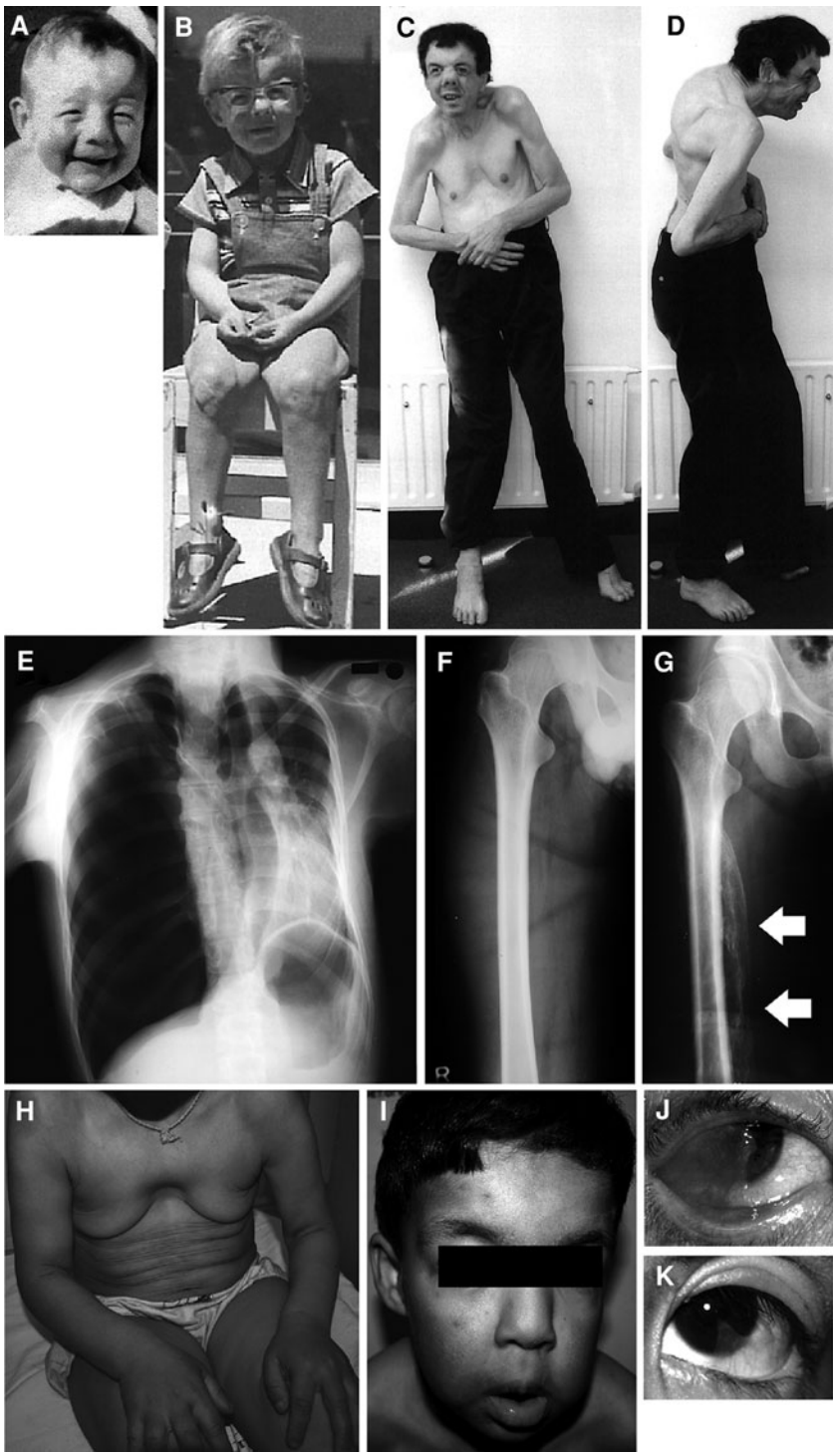

Fig. 1 Clinical variability and progression of *ATP6V0A2*-related ARCL. **a**–**d** Progressive phenotype of the oldest *ATP6V0A2*-related ARCL patient described so far. At the age of one (**a**) and five (**b**) patient 2 presented with facial features typical for this type of ARCL, but no obvious asymmetry of spine or extremities. **c**, **d** At the age of 40 years the same individual shows a progression of the facial dysmorphism as well as kyphoscoliosis. Differences between leg length and shoulder position are due to chronic luxations. **e**–**g** Radiological investigations of patient 2. **e** At the age of 16 years he displayed a pneumothorax of the right lung, a luxation of the right shoulder, and a scoliosis of the thoracic vertebral column. **f** X-ray at the age of 19 years showing grossly normal configuration of the femur. **g** Less than a year later heterotopic calcifications (*arrows*) surrounding the femur had developed. **h**, **i** At five years of age patient 8 of Indian origin showed the typical facial appearance as well as persistent abdominal wrinkling and sagging of the skin while skin wrinkling is absent at the dorsum of the hands. **j** Eye of 40-year-old patient 2 showing pterygium. **k** Eye of patient 8 showing beginning pterygium

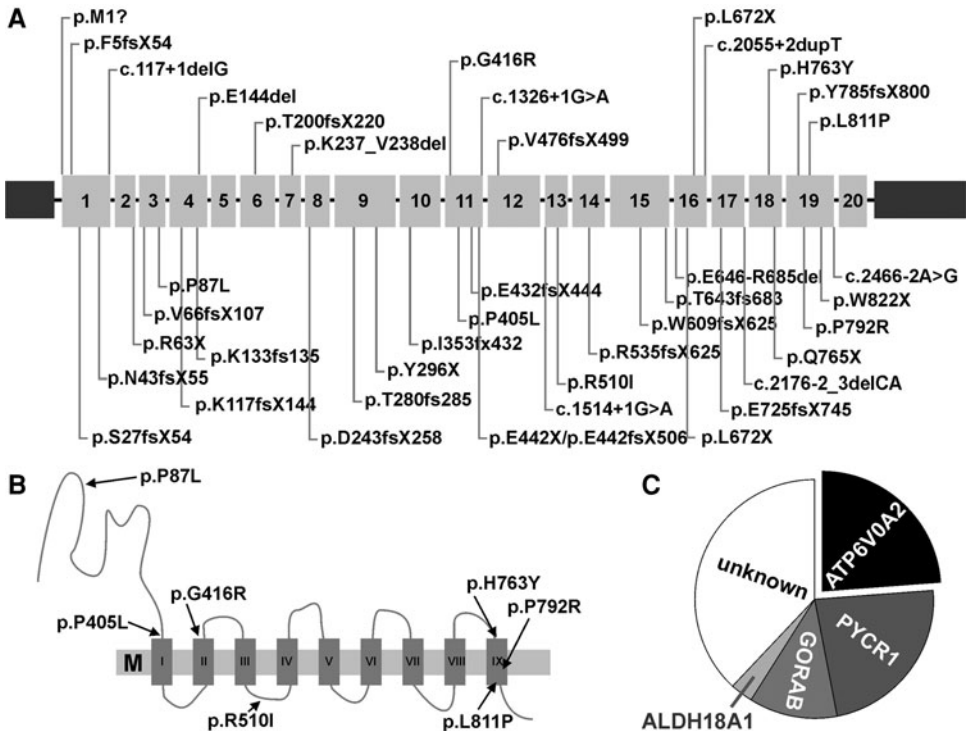

Fig. 2 Mutational spectrum of *ATP6V0A2*-related cutis laxa. **a** Schematic overview of all known *ATP6V0A2* mutations. On *top* of the exon overview, all mutations identified in the present study are shown. *Below* all mutations described so far are shown (Hucthagowder et al. 2009; Kornak et al. 2008). No accumulation in a hotspot is visible. **b** All known missense mutations are indicated on a schematic view of the ATP6V0A2 protein integrated in the membrane (*M*). Also here no clustering of the known mutations is detectable. **c** Frequency of mutations in ARCL2-associated genes in our current cohort. From 211 affected individuals 24 % carry *ATP6V0A2*, 23 % *PYCR1*, 12 % *GORAB* and 3 % *ALDH18A1* mutations. One patient showed a RIN2 mutation. In 38 % the molecular cause for the ARCL phenotype is not yet identified

12) were described previously (Hucthagowder et al. 2009; Kornak et al. 2008). All other mutations identified in this study are novel. Patients 1, 5, 7 and 13 are compound heterozygous. On genomic as well as cDNA level only one heterozygous mutation was detected in patient 2. However, a pronounced nonsense-mediated decay of the *ATP6V0A2* mRNA in fibroblasts corroborated an *ATP6V0A2*-related ARCL2 (Supplementary Fig. 1a). The second mutation most probably resides in non-coding regions not included in the mutation screening.

A comparison of all described *ATP6V0A2* mutations (Fig. 2a, lower part) with our newly identified alterations (Fig. 2a, upper part) shows no accumulation in specific regions of the gene. The majority of the mutations leads to truncations and thus underline the hypothesis that the basis of *ATP6V0A2*-related CL is a loss of function by a loss of protein. Evaluation using the program MutationTaster (Schwarz et al. 2010) showed that the residues affected by missense mutations are evolutionarily highly conserved and therefore probably functionally important. While G416 is at the beginning of the putative transmembrane helix 2; H763 and L811 resides in and at the end of the last transmembrane helix, respectively. Residue P87 lies inside the cytoplasmatic N-terminal tail, whereas R510 is localized in a luminal loop (Fig. 2b).

Up to now our ARCL research network has collected 211 affected individuals from 183 families without obvious lung involvement, which qualifies them as ARCL type 2. Of these individuals, 24 % had mutations in *ATP6V0A2*, 23 % in *PYCR1* and 12 % in *GORAB*. Furthermore, seven patients (3 %) harboured mutations in *ALDH18A1* and one in *RIN2*. In the remaining 38 % the genetic defect is still unknown (Fig. 2c).

Localization of ATP6V0A2 within the Golgi compartment

Whereas morphological and functional alterations of the Golgi compartment induced by ATP6V0A2-deficiency imply a Golgi-localization, previous studies primarily detected the protein in early endosomes (Hurtado-Lorenzo et al. 2006). In order to clarify the localisation in a cell type relevant for the CL phenotype, we performed immunostaining using an antibody against ATP6V0A2. In control cells the antibody stained a structure in a juxtanuclear position, co-localizing with different Golgi marker proteins

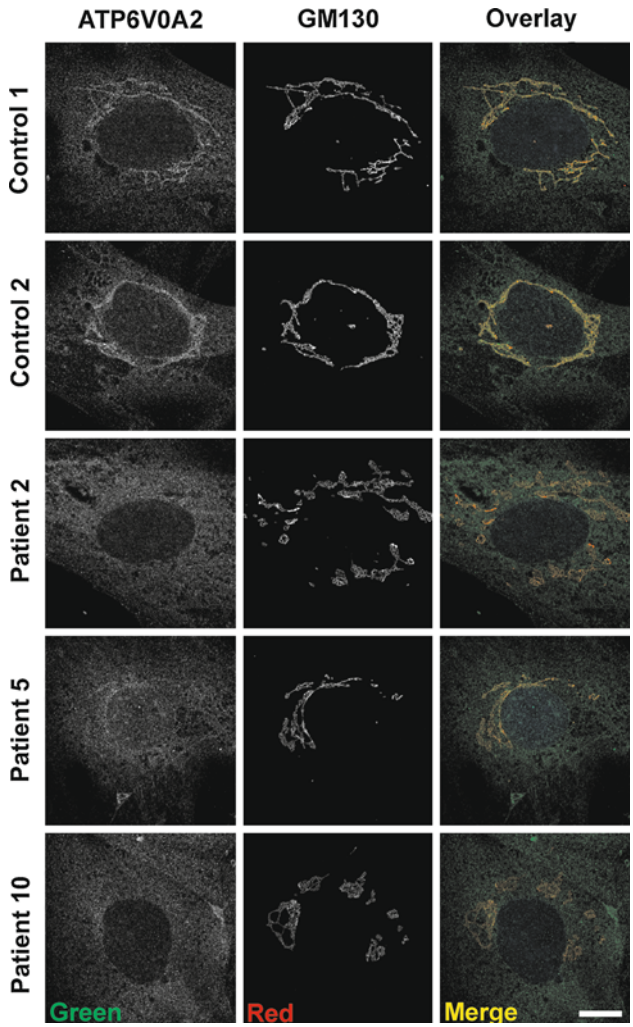

Fig. 3 Subcellular localization of ATP6V0A2 and its loss in patients' fibroblasts. Immunolabelling of control skin fibroblasts with an antibody against the N-terminal domain of ATP6V0A2 (*green*). A perinuclear localization is visible in *Control 1* as well as *Control 2*. Staining of GM130 (*red*), a protein localized in the *cis*-Golgi apparatus, revealed a similar structure. A co-localization of both signals is detectable indicating a localization of ATP6V0A2 in the Golgi apparatus. In patient-derived fibroblasts, an altered GM130-positive structure is evident. No green signal was detectable in cells from patient 2 and 10 indicating a loss of ATP6V0A2. In cells from patient 5 minor labelling is detectable co-localizing with GM130. *Scale bar* 10 µm (color figure online)

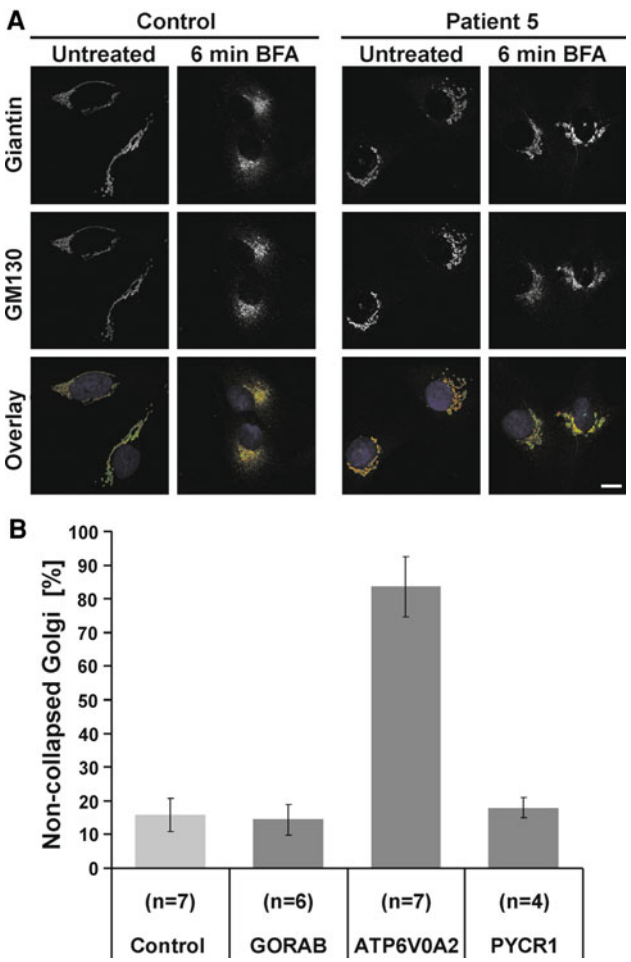

Fig. 4 Specificity of delayed Golgi collapse after brefeldin A treatment. **a** Representative images of control and patient fibroblasts untreated or treated with 5 µg/ml brefeldin A for 6 min. Cells where stained for giantin (*green*) and GM130 (*red*). Control cells with completely collapsed Golgi structure and cells from patient 5 with almost unchanged Golgi morphology are shown. *Scale bar* 10 µm. **b** After 5 µg/ml brefeldin A treatment for 6 min staining for GM130 and giantin revealed non-collapsed Golgi structures in around 20 % of control, *GORAB*-, and *PYCR1*-deficient cells versus around 80 % in *ATP6V0A2*-deficient cells (color figure online)

(Fig. 3), proving that the a2 subunit of the V-Type H^+-ATPase is localized at the Golgi apparatus.

Next, skin fibroblasts from three CL affected individuals with different *ATP6V0A2* mutations were examined (Fig. 3). In cells from patients 2 and 10 no ATP6V0A2 fluorescence staining was detectable at the Golgi apparatus. A mild to severe fragmentation of the Golgi structure was observed as described previously (Hucthagowder et al. 2009). In cells from patient 5 some ATP6V0A2 Golgi staining was still visible. This patient carries a splice site mutation on one allele, predicted to result in a premature termination of the protein. The p.L811P mutation on the other allele is likely to result in a partially stable protein.

Brefeldin A-induced Golgi collapse

By binding to ARF-GEFs brefeldin A (BFA) leads to ARF1 dysregulation (Hendricks et al. 1992; Steet and Kornfeld 2006). As a consequence, the formation of tubules is induced that connect Golgi compartment and endoplasmic reticulum (ER), thus disturbing the equilibrium between antero- and retrograde transport between both compartments. ATP6V0A2 deficiency has been described to delay the resulting collapse of the Golgi

compartment triggered by BFA (Kornak et al. 2008). We extended this study and included skin fibroblasts from ARCL patients carrying mutations in the genes *ATP6V0A2*, *GORAB*, and *PYCR1* in order to determine if this is a common feature of ARCL gene defects. Golgi integrity after 6 min BFA treatment was assessed by counting cells stained for giantin (Fig. 4a). In control cells 80 % of the giantin signal was completely dispersed while in fibroblasts carrying *ATP6V0A2* mutations 90 % of the cells showed remaining Golgi structures. Cells carrying mutations in *GORAB* or *PYCR1* behaved like control cells (Fig. 4b).

We reproduced these effects in HeLa cells after knock-down of *ATP6V0A2*, *GORAB* and *PYCR1* by siRNA. Efficiency of the knock-down was corroborated by quantitative PCR (Supplementary Fig. 1b). After treatment with BFA for different time points again only ATP6V0A2-deficient cells showed a delayed Golgi collapse. After 10 min in almost 80 % of GORAB- and PYCR1-deficient cells Golgi structures were dispersed, whereas in more than 60 % of ATP6V0A2-depleted cells Golgi morphology remained comparable to untreated cells (Supplementary Fig. 2). This corroborates that this effect is unique for *ATP6V0A2*-related ARCL.

Altered TGF-β signalling

In several connective tissue disorders TGF-β signalling was shown to be altered (Callewaert et al. 2011; ten Dijke and Arthur 2007). We wanted to know whether this also applies to *ATP6V0A2*-related ARCL. Skin fibroblasts from patients and control individuals were cultivated 3 days past confluency before TGF-β signalling was determined by detection of P-Smad2, which is phosphorylated upon activation of the TGF-β receptor type 1. Quantification showed on average a twofold higher Smad2 phosphorylation in ATP6V0A2-deficient cells compared to controls (Fig. 5a). In order to investigate the basis of this effect we measured total TGF-β1 in cell culture supernatants and found a clear elevation (Fig. 5b). However, we could not detect any increase in active TGF-β1. There was no evidence for a transcriptional *TGFB1* upregulation (Supplementary Fig. 3). This demonstrates an increased availability of latent TGF-β1 in spite of normal gene transcription.

Discussion

Within the last years, the genetic basis of several autosomal recessive syndromes with cutis laxa was elucidated, which greatly facilitates the distinction of these clinically overlapping syndromes (Basel-Vanagaite et al. 2009; Hennies et al. 2008; Kornak et al. 2008; Morava et al. 2009a; Reversade et al. 2009; Urban et al. 2009). In the present

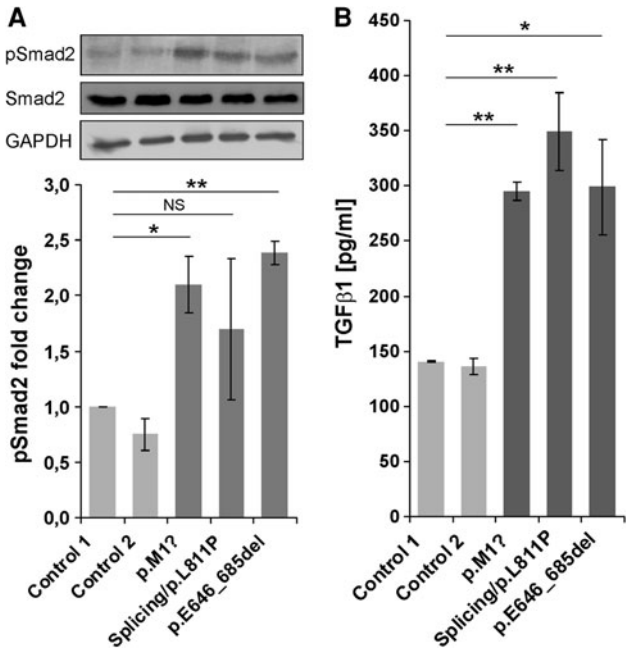

Fig. 5 TGF-β signalling in ATP6V0A2-deficient skin fibroblasts. **a** Analysis of Smad2 phosphorylation in ATP6V0A2-deficient skin fibroblasts. Cells were cultivated for 3 days after confluency, lysed and subsequently analyzed by immunoblot. A significant increase in Smad2 phosphorylation was detectable in fibroblasts from three patients, whereas Smad2 and GAPDH protein levels remained unchanged (representative result). Quantification of the results of three independent experiments showed on average a twofold increase of Smad2 phosphorylation. **b** Quantification by an ELISA for active TGF-β1 showed a twofold increase in supernatants from ATP6V0A2-deficient fibroblasts relative to control cells after acid activation of TGF-β1. Values are the average of two independent experiments. Students *t* test revealed *p* values: $*p < 0.005$; $**p < 0.0005$

study we examined 13 patients with clear signs of ARCL2A, Debré type, or wrinkly skin syndrome. All patients selected for mutation analysis based on major diagnostic features, presented with lax and wrinkled skin, joint laxity, often leading to hip dislocations, and a large fontanel with late closure. In contrast to *ALDH18A1*- and *PYCR1*-related ARCL severe intrauterine growth retardation was rarely noted, birth weights were usually between the 10th and 25th percentiles. All patients showed a specific facial gestalt. In addition to the previously described downslanting palpebral fissures and broad nasal root, they had a typical distribution of sagging supraorbital skin and a long face. In some patients other important discriminating features are the previously described cobblestone-like brain malformation and the combined CDG type II N-glycosylation and O-glycosylation defect, which was evident in all patients analyzed (Morava et al. 2009b; Gardeitchik et al., in preparation).

Patient 2 is of special interest as he is the oldest individual with an *ATP6V0A2* mutation described so far and showed a strikingly progressive phenotype leading to

kyphoscoliosis and facial coarsening. He also had a mild to moderate mental retardation and seizures without progression. These features are reminiscent of MACS patients with *RIN2* mutations (Basel-Vanagaite et al. 2009; Mohamed et al. 2011a). The use of TIEF was therefore very important for discriminating between the two disorders. Furthermore, heterotopic calcifications of muscle and connective tissue developed in patient 2 between the age of 19 and 26. No pain or indurations were reported at these sites and the origin remains unclear. A combination of cutis laxa with pathologic calcifications is observed in pseudoxanthoma elasticum (PXE) and related disorders that affect gamma carboxylation of mineralisation inhibitors (Kornak 2011; Vanakker et al. 2011). However, in these disorders calcifications are usually found in skin, kidneys and the vascular system, not in muscles or tendons. Patient 2 as well as patient 8 displayed an ophthalmic pterygium at one eye. Pterygia typically appear in adults and possibly involve somatic changes in oncogenes (KRAS, TP53), growth factors and canonical WNT-signalling (Detorakis and Spandidos 2009). Therefore, the exceptional appearance of a pterygium in childhood might be an interesting aspect for the understanding of the pathogenesis of *ATP6V0A2*-related ARCL. All these features have never been described before in *ATP6V0A2*-related ARCL and it remains to be determined how frequent they become when patients grow older.

Mutation screening in patient 2 only revealed one heterozygous, clearly pathogenic mutation, but strong nonsense-mediated decay of *ATP6V0A2* mRNA, absence of the protein, altered TIEF patterns and the typical behaviour in the BFA-assay underlined that ATP6V0A2 deficiency is the cause of the disorder. All *ATP6V0A2* mutations described so far have been classified as loss-of-function mutations (Kornak et al. 2008). The present study identified 17 *ATP6V0A2* mutations either leading to altered splicing or to premature protein termination. No clustering within a hotspot was detectable. Missense mutations are rare events in *ATP6V0A2*-related ARCL, representing only 17 % of all mutations. The alterations on position P405 and G416 are localized in the first, whereas H763, P792 and L811 are localized in the last putative transmembrane helix of the ATP6V0A2 protein. These mutations might cause misfolding or a disturbed insertion into the membrane. In the a subunit of *S. cerevisiae* both regions of the protein have been implicated in assembly of the V-ATPase complex (Kawasaki-Nishi et al. 2003). Therefore, an alteration of this position could lead to a stable protein unable to transport protons. Within our cohort of 211 affected individuals *ATP6V0A2* mutations are the most common cause of ARCL. The second and third most frequently affected genes are *PYCR1* and *GORAB*, respectively. This information might be important for the prioritization of candidate genes in a diagnostic approach for ARCL.

The V-type H^+-ATPase is present in multiple tissues and in several subcellular compartments (Guillard et al. 2009; Jefferies et al. 2008). For the ATPase complex assembled around the a2 subunit two different subcellular localizations have been described: the Golgi compartment and the early endosomes (Hurtado-Lorenzo et al. 2006; Sun-Wada et al. 2011). We detected a clear Golgi localization of this protein in human dermal fibroblasts, the cell type most likely responsible for the ARCL skin manifestations. An additional localization in early endosomes or other parts of the endocytic pathway cannot be excluded due to the low signal strength of the antibody. As expected, the mutation in patients 2 and 10 resulted in an absence of the protein while in patient 5, carrying a heterozygous splice site mutation as well as a heterozygous missense mutation, weak labelling was detectable. This corroborates the suggested loss-of-function effect of *ATP6V0A2* mutations.

We described that cells deficient for ATP6V0A2 show a delayed collapse of the Golgi compartment upon treatment with BFA (Kornak et al. 2008). In the current study we extended this initial observation and included skin fibroblasts with different known ARCL defects to better evaluate its role in ARCL pathogenesis and its value as a diagnostic test within the spectrum of ARCL. Only ATP6V0A2-, but not GORAB- or PYCR1-deficient skin fibroblasts and HeLa cells showed this delay. Thus if patient fibroblasts are available, testing disassembly of the Golgi apparatus induced by BFA provides a simple and quick possibility to pre-screen for ATP6V0A2 deficiency. This specificity is especially surprising since GORAB, the protein mutated in gerodermia osteodysplastica (GO), interacts with Rab6, a bona fide regulator of retrograde trafficking within the secretory pathway (Hennies et al. 2008). So far, *COG7* mutations are the only other defect linked with a delayed Golgi collapse after BFA treatment associated with CL (Morava et al. 2007; Steet and Kornfeld 2006; Wu et al. 2004). This phenotype can be easily differentiated from *ATP6V0A2*-related ARCL due to its severity and early lethality. Interestingly, COG7-deficient patients also show CDG-specific features, but GO patients do not (Rajab et al. 2008; Wu et al. 2004). As it was demonstrated that the COG complex plays a role in fusion of intra-Golgi vesicles that transport glycosylation enzymes to ensure their correct position in the Golgi stack a similar role might also apply for ATP6V0A2 (Shestakova et al. 2006). However, the mechanism seems to be slightly different. While COG-deficiency delays the onset of BFA-induced tubule formation at the Golgi, disruption of the pH gradient slows down the extension of these tubules (Barzilay et al. 2005; Flanagan-Steet et al. 2011). In spite of considerable expression and correct Golgi localization of the mutated a2 subunit in fibroblasts from patient 5 the

delay of BFA-induced trafficking was in the usual range for *ATP6V0A2*-related ARCL. It can be speculated that the p.L811P exchange disturbs formation of the last helix and therefore impairs either interaction with other subunits, proton translocation, or both (Nishi and Forgac 2002).

We found elevated levels of latent TGF-β1 in ARCL2 skin fibroblast cell culture supernatant and upregulated TGF-β downstream signalling. As already reported by Saito et al., active TGF-β1 was below the detection threshold in supernatants from skin fibroblasts (Saito et al. 2001). Surprisingly, although an autoregulatory loop regulating *TGFB1* had been described previously (Bascom et al. 1989) we found no increased *TGFB1* gene expression. In several syndromes with impaired extracellular matrix (ECM) formation with cardiovascular involvement, including forms of autosomal dominant and autosomal recessive cutis laxa, TGF-β signalling was shown to be upregulated (Callewaert et al. 2011; Dietz 2010; Hoyer et al. 2009; Urban et al. 2009). Using a cell-based assay LTBP4 deficiency was shown to entail an approximately threefold increase in active TGF-β in fibroblasts from patients with Urban–Rifkin–Davis syndrome, which is in the same range as our results (Urban et al. 2009). LTBPs are part of the large latency complex, which anchors latent TGF-β to the ECM (Annes et al. 2003). Therefore, increased bioavailability of latent TGF-β can be due to both, an impairment of LTBPs or of the ECM. Accordingly, fibroblasts expressing mutant elastin displayed strongly increased TGF-β signalling (Callewaert et al. 2011). In contrast, previous results showed normal elastin deposition by ATP6V0A2-deficient fibroblasts at the time point (3 days after confluency) at which we measured TGF-β1 (Hucthagowder et al. 2009). Whether disturbed LTBP function could be an explanation remains to be determined.

In cell types with a predominant endosomal localization of ATP6V0A2 a role of this subunit in endocytosis was shown (Hurtado-Lorenzo et al. 2006). A delay of endocytosis was shown to enhance Smad2 phosphorylation upon addition of TGF-β (Chen 2009). Under the assumption of a significant endosomal function of ATP6V0A2 in skin fibroblasts delayed endocytosis could therefore explain enhanced TGF-β downstream signalling independent of increased levels of latent TGF-β. Further research is necessary to clarify this point.

Web resources

Online Mendelian Inheritance in Man (OMIM) http://www.ncbi.nlm.gov/Omim/ (for OHS, ADCL and ARCL1 and ARCL2A, ARCL2B, DBS, MACS).

Acknowledgments We are grateful to the patients and their family members whose cooperation made this study possible. We would like to thank the family of patient 2 especially for their great contribution and interest in our work. We thank Traute Burmester for her excellent help with fibroblast cultivation from skin biopsies. We additionally thank E. Ntrivalas for providing the ATP6V0A2 antibody. This study was funded by the Fritz Thyssen Stiftung to Uwe Kornak.

Conflict of interest The authors declare no conflict of interest.

References

Albrecht B, de Brouwer AP, Lefeber DJ, Cremer K, Hausser I, Rossen N, Wortmann SB, Wevers RA, Kornak U, Morava E (2011) MACS syndrome: a combined collagen and elastin disorder due to abnormal Golgi trafficking. Am J Med Genet A 152A:2916–2918

Annes JP, Munger JS, Rifkin DB (2003) Making sense of latent TGFβ activation. J Cell Sci 116:217–224

Barzilay E, Ben-Califa N, Hirschberg K, Neumann D (2005) Uncoupling of brefeldin a-mediated coatomer protein complex-I dissociation from Golgi redistribution. Traffic 6:794–802. doi:10.1111/j.1600-0854.2005.00317.x

Bascom CC, Wolfshohl JR, Coffey RJ Jr, Madisen L, Webb NR, Purchio AR, Derynck R, Moses HL (1989) Complex regulation of transforming growth factor beta 1, beta 2, and beta 3 mRNA expression in mouse fibroblasts and keratinocytes by transforming growth factors beta 1 and beta 2. Mol Cell Biol 9:5508–5515

Basel-Vanagaite L, Sarig O, Hershkovitz D, Fuchs-Telem D, Rapaport D, Gat A, Isman G, Shirazi I, Shohat M, Enk CD, Birk E, Kohlhase J, Matysiak-Scholze U, Maya I, Knopf C, Peffekoven A, Hennies HC, Bergman R, Horowitz M, Ishida-Yamamoto A, Sprecher E (2009) RIN2 deficiency results in macrocephaly, alopecia, cutis laxa, and scoliosis: MACS syndrome. Am J Hum Genet 85:254–263

Beyenbach KW, Wieczorek H (2006) The V-type H+ ATPase: molecular structure and function, physiological roles and regulation. J Exp Biol 209:577–589

Bicknell LS, Pitt J, Aftimos S, Ramadas R, Maw MA, Robertson SP (2008) A missense mutation in ALDH18A1, encoding Delta1-pyrroline-5-carboxylate synthase (P5CS), causes an autosomal recessive neurocutaneous syndrome. Eur J Hum Genet 16:1176–1186

Callewaert B, Renard M, Hucthagowder V, Albrecht B, Hausser I, Blair E, Dias C, Albino A, Wachi H, Sato F, Mecham RP, Loeys B, Coucke PJ, De Paepe A, Urban Z (2011) New insights into the pathogenesis of autosomal-dominant cutis laxa with report of five ELN mutations. Hum Mutat 32:445–455

Chen YG (2009) Endocytic regulation of TGF-β signaling. Cell Res 19:58–70. doi:10.1038/cr.2008.315

de Barsy AM, Moens E, Dierckx L (1968) Dwarfism, oligophrenia and degeneration of the elastic tissue in skin and cornea. A new syndrome? Helv Paediatr Acta 23:305–313

Detorakis ET, Spandidos DA (2009) Pathogenetic mechanisms and treatment options for ophthalmic pterygium: trends and perspectives (review). Int J Mol Med 23:439–447

Dietz HC (2010) TGF-β in the pathogenesis and prevention of disease: a matter of aneurysmic proportions. J Clin Invest 120:403–407. doi:10.1172/JCI42014

Flanagan-Steet H, Johnson S, Smith RD, Bangiyeva J, Lupashin V, Steet R (2011) Mislocalization of large ARF-GEFs as a potential

mechanism for BFA resistance in COG-deficient cells. Exp Cell Res 317:2342–2352. doi:10.1016/j.yexcr.2011.06.005

Guillard M, Dimopoulou A, Fischer B, Morava E, Lefeber DJ, Kornak U, Wevers RA (2009) Vacuolar H+-ATPase meets glycosylation in patients with cutis laxa. Biochim Biophys Acta 1792:903–914

Hendricks LC, McClanahan SL, McCaffery M, Palade GE, Farquhar MG (1992) Golgi proteins persist in the tubulovesicular remnants found in brefeldin A-treated pancreatic acinar cells. Eur J Cell Biol 58:202–213

Hennies HC, Kornak U, Zhang H, Egerer J, Zhang X, Seifert W, Kuhnisch J, Budde B, Natebus M, Brancati F, Wilcox WR, Muller D, Kaplan PB, Rajab A, Zampino G, Fodale V, Dallapiccola B, Newman W, Metcalfe K, Clayton-Smith J, Tassabehji M, Steinmann B, Barr FA, Nurnberg P, Wieacker P, Mundlos S (2008) Gerodermia osteodysplastica is caused by mutations in SCYL1BP1, a Rab-6 interacting golgin. Nat Genet 40:1410–1412

Hoyer J, Kraus C, Hammersen G, Geppert JP, Rauch A (2009) Lethal cutis laxa with contractural arachnodactyly, overgrowth and soft tissue bleeding due to a novel homozygous fibulin-4 gene mutation. Clin Genet 76:276–281

Hucthagowder V, Sausgruber N, Kim KH, Angle B, Marmorstein LY, Urban Z (2006) Fibulin-4: a novel gene for an autosomal recessive cutis laxa syndrome. Am J Hum Genet 78:1075–1080

Hucthagowder V, Morava E, Kornak U, Lefeber DJ, Fischer B, Dimopoulou A, Aldinger A, Choi J, Davis EC, Abuelo DN, Adamowicz M, Al-Aama J, Basel-Vanagaite L, Fernandez B, Greally MT, Gillessen-Kaesbach G, Kayserili H, Lemyre E, Tekin M, Turkmen S, Tuysuz B, Yuksel-Konuk B, Mundlos S, Van Maldergem L, Wevers RA, Urban Z (2009) Loss-of-function mutations in ATP6V0A2 impair vesicular trafficking, tropoelastin secretion and cell survival. Hum Mol Genet 18:2149–2165

Hurtado-Lorenzo A, Skinner M, El Annan J, Futai M, Sun-Wada GH, Bourgoin S, Casanova J, Wildeman A, Bechoua S, Ausiello DA, Brown D, Marshansky V (2006) V-ATPase interacts with ARNO and Arf6 in early endosomes and regulates the protein degradative pathway. Nat Cell Biol 8:124–136

Jefferies KC, Cipriano DJ, Forgac M (2008) Function, structure and regulation of the vacuolar (H+)-ATPases. Arch Biochem Biophys 476:33–42

Kawasaki-Nishi S, Nishi T, Forgac M (2003) Proton translocation driven by ATP hydrolysis in V-ATPases. FEBS Lett 545:76–85

Kornak U (2011) Animal models with pathological mineralization phenotypes. Jt Bone Spine 78:561–567. doi:10.1016/j.jbspin.2011.03.020

Kornak U, Reynders E, Dimopoulou A, van Reeuwijk J, Fischer B, Rajab A, Budde B, Nurnberg P, Foulquier F, Lefeber D, Urban Z, Gruenewald S, Annaert W, Brunner HG, van Bokhoven H, Wevers R, Morava E, Matthijs G, Van Maldergem L, Mundlos S (2008) Impaired glycosylation and cutis laxa caused by mutations in the vesicular H+-ATPase subunit ATP6V0A2. Nat Genet 40:32–34

Kunze J, Majewski F, Montgomery P, Hockey A, Karkut I, Riebel T (1985) De Barsy syndrome—an autosomal recessive, progeroid syndrome. Eur J Pediatr 144:348–354

Loeys B, Van Maldergem L, Mortier G, Coucke P, Gerniers S, Naeyaert JM, De Paepe A (2002) Homozygosity for a missense mutation in fibulin-5 (FBLN5) results in a severe form of cutis laxa. Hum Mol Genet 11:2113–2118

McHenry P, Wang WL, Devitt E, Kluesner N, Davisson VJ, McKee E, Schweitzer D, Helquist P, Tenniswood M (2010) Iejimalides A and B inhibit lysosomal vacuolar H+-ATPase (V-ATPase) activity and induce S-phase arrest and apoptosis in MCF-7 cells. J Cell Biochem 109:634–642

Mohamed M, Guillard M, Wortmann SB, Cirak S, Marklova E, Michelakakis H, Korsch E, Adamowicz M, Koletzko B, van Spronsen FJ, Niezen-Koning KE, Matthijs G, Gardeitchik T, Kouwenberg D, Lim BC, Zeevaert R, Wevers RA, Lefeber DJ, Morava E (2011a) Clinical and diagnostic approach in unsolved CDG patients with a type 2 transferrin pattern. Biochim Biophys Acta 1812:691–698. doi:10.1016/j.bbadis.2011.02.011

Mohamed M, Kouwenberg D, Gardeitchik T, Kornak U, Wevers RA, Morava E (2011b) Metabolic cutis laxa syndromes. J Inherit Metab Dis 34:907–916. doi:10.1007/s10545-011-9305-9

Morava E, Wopereis S, Coucke P, Gillessen-Kaesbach G, Voit T, Smeitink J, Wevers R, Grunewald S (2005) Defective protein glycosylation in patients with cutis laxa syndrome. Eur J Hum Genet 13:414–421

Morava E, Zeevaert R, Korsch E, Huijben K, Wopereis S, Matthijs G, Keymolen K, Lefeber DJ, De Meirleir L, Wevers RA (2007) A common mutation in the COG7 gene with a consistent phenotype including microcephaly, adducted thumbs, growth retardation, VSD and episodes of hyperthermia. Eur J Hum Genet 15:638–645

Morava E, Guillard M, Lefeber DJ, Wevers RA (2009a) Autosomal recessive cutis laxa syndrome revisited. Eur J Hum Genet 17:1099–1110

Morava E, Wevers RA, Willemsen MA, Lefeber D (2009b) Cobblestone-like brain dysgenesis and altered glycosylation in congenital cutis laxa, Debre type. Neurology 73:1164 (author reply 1164–1165)

Nishi T, Forgac M (2002) The vacuolar (H+)-ATPases—nature's most versatile proton pumps. Nat Rev Mol Cell Biol 3:94–103

Noordam C, Funke S, Knoers NV, Jira P, Wevers RA, Urban Z, Morava E (2009) Decreased bone density and treatment in patients with autosomal recessive cutis laxa. Acta Paediatr 98:490–494

Ntrivalas E, Gilman-Sachs A, Kwak-Kim J, Beaman K (2007) The N-terminus domain of the a2 isoform of vacuolar ATPase can regulate interleukin-1β production from mononuclear cells in co-culture with JEG-3 choriocarcinoma cells. Am J Reprod Immunol 57:201–209

Rajab A, Kornak U, Budde BS, Hoffmann K, Jaeken J, Nurnberg P, Mundlos S (2008) Geroderma osteodysplasticum hereditaria and wrinkly skin syndrome in 22 patients from Oman. Am J Med Genet A 146A:965–976

Reversade B, Escande-Beillard N, Dimopoulou A, Fischer B, Chng SC, Li Y, Shboul M, Tham PY, Kayserili H, Al-Gazali L, Shahwan M, Brancati F, Lee H, O'Connor BD, Schmidt-von Kegler M, Merriman B, Nelson SF, Masri A, Alkazaleh F, Guerra D, Ferrari P, Nanda A, Rajab A, Markie D, Gray M, Nelson J, Grix A, Sommer A, Savarirayan R, Janecke AR, Steichen E, Sillence D, Hausser I, Budde B, Nurnberg G, Nurnberg P, Seemann P, Kunkel D, Zambruno G, Dallapiccola B, Schuelke M, Robertson S, Hamamy H, Wollnik B, Van Maldergem L, Mundlos S, Kornak U (2009) Mutations in PYCR1 cause cutis laxa with progeroid features. Nat Genet 41:1016–1021

Saito T, Kinoshita A, Yoshiura K, Makita Y, Wakui K, Honke K, Niikawa N, Taniguchi N (2001) Domain-specific mutations of a transforming growth factor (TGF)-β 1 latency-associated peptide cause Camurati–Engelmann disease because of the formation of a constitutively active form of TGF-β 1. J Biol Chem 276:11469–11472. doi:10.1074/jbc.C000859200

Schwarz JM, Rodelsperger C, Schuelke M, Seelow D (2010) MutationTaster evaluates disease-causing potential of sequence alterations. Nat Methods 7:575–576

Shestakova A, Zolov S, Lupashin V (2006) COG complex-mediated recycling of Golgi glycosyltransferases is essential for normal protein glycosylation. Traffic 7:191–204

Steet R, Kornfeld S (2006) COG-7-deficient human fibroblasts exhibit altered recycling of Golgi proteins. Mol Biol Cell 17:2312–2321

Sun-Wada GH, Tabata H, Kuhara M, Kitahara I, Takashima Y, Wada Y (2011) Generation of chicken monoclonal antibodies against the a1, a2, and a3 subunit isoforms of vacuolar-type proton ATPase. Hybridoma (Larchmt) 30:199–203

ten Dijke P, Arthur HM (2007) Extracellular control of TGFβ signalling in vascular development and disease. Nat Rev Mol Cell Biol 8:857–869

Urban Z, Hucthagowder V, Schurmann N, Todorovic V, Zilberberg L, Choi J, Sens C, Brown CW, Clark RD, Holland KE, Marble M, Sakai LY, Dabovic B, Rifkin DB, Davis EC (2009) Mutations in LTBP4 cause a syndrome of impaired pulmonary, gastrointestinal, genitourinary, musculoskeletal, and dermal development. Am J Hum Genet 85:593–605

Van Maldergem L, Yuksel-Apak M, Kayserili H, Seemanova E, Giurgea S, Basel-Vanagaite L, Leao-Teles E, Vigneron J, Foulon M, Greally M, Jaeken J, Mundlos S, Dobyns WB (2008) Cobblestone-like brain dysgenesis and altered glycosylation in congenital cutis laxa, Debre type. Neurology 71:1602–1608

Vanakker OM, Leroy BP, Schurgers LJ, Vermeer C, Coucke PJ, De Paepe A (2011) Atypical presentation of pseudoxanthoma elasticum with abdominal cutis laxa: evidence for a spectrum of ectopic calcification disorders? Am J Med Genet A 155A:2855–2859. doi:10.1002/ajmg.a.34264

Wu X, Steet RA, Bohorov O, Bakker J, Newell J, Krieger M, Spaapen L, Kornfeld S, Freeze HH (2004) Mutation of the COG complex subunit gene COG7 causes a lethal congenital disorder. Nat Med 10:518–523